



## Concept paper

# Different flavors of diffusion in paramagnetic systems: Unexpected NMR signal intensity and relaxation enhancements

Enrico Ravera<sup>a,b</sup>, Marco Fragai<sup>a,b</sup>, Giacomo Parigi<sup>a,b</sup>, Claudio Luchinat<sup>a,b,\*</sup>

<sup>a</sup> Magnetic Resonance Center (CERM) and Interuniversity Consortium for Magnetic Resonance of Metallo Proteins (CIRMMMP), Via L. Sacconi 6, 50019 Sesto Fiorentino, Italy

<sup>b</sup> Department of Chemistry “Ugo Schiff”, University of Florence, Via della Lastruccia 3, 50019 Sesto Fiorentino, Italy



## ARTICLE INFO

## Keywords:

MRI contrast agents  
DNP  
hyperpolarization  
Overhauser  
spin diffusion

## ABSTRACT

The NMR community is well acquainted with different kinds of diffusion but, at the same time, there are several effects that are worth a better understanding for an improved design of molecular imaging and dynamic nuclear polarization experiments. Spin diffusion and chemical diffusion are known to play important roles in determining the NMR signal and relaxation enhancements caused by the presence of paramagnetic molecules in solution. Paramagnetic complexes are used as contrast agents in magnetic resonance imaging, due to their efficacy in selectively increase the relaxation rates of solvent water protons, as well as in dynamic nuclear polarization experiments to increase the NMR signal of desired molecules through polarization transfer from unpaired electrons. In this paper we review some recent, unexpected observations in these two areas, which seem related to spin and/or chemical diffusion, and demonstrate the need for a detailed understanding of the interplay of different phenomena. A deeper understanding of spin and chemical diffusion may thus result very important for an improved design of contrast agents for magnetic resonance imaging and for the optimization of hyperpolarization experiments.

## 1. Introduction

Since NMR is an intrinsically insensitive technique, especially in low field applications, different methods have been explored to maximize the signal-to-noise per unit time, as well as to increase the spatial resolution among different compartments. In both cases, paramagnetic agents are the method of choice, because they can be used to increase the signal beyond thermal population through dynamic nuclear polarization (DNP) and because they can be used to tune the shift and relaxation of abundant molecules (water, in general) to increase the contrast among different kind of tissues in Magnetic Resonance Imaging (MRI). In both cases, over the years the experimental design has been in some sense standardized, and “recipes” are available for researchers that aim at further improving the experiments, in terms of radical/contrast agent design, formulation design etc. However, there are some notable cases where unexpected results arise. Quite often, these results are not directly linked to the nature of the paramagnetic centers, but rather to (spin and chemical) diffusion properties of the environment in which they perform their task.

Chemical diffusion has profound effects on NMR properties, and therefore represents a topic of great importance in modern magnetic resonance. NMR can be used to measure diffusion coefficients and to

resolve different compounds spectroscopically in a mixture, taking advantage of their different diffusion. Here, we focus on the effects of diffusion on some selected applications pertaining paramagnetic systems, and thus diffusion NMR experiments are not covered. We refer the interested reader to references [1–4].

## 2. MRI contrast agents: surprises are still possible

MRI often requires the use of contrast agents for high resolution images with a good contrast between different tissues or compartments [5–10]. The complexes presently used in clinical analysis are suboptimal in terms of increase of the contrast (which is proportional to the relaxation enhancement that they induce in solvent water protons), biodistribution, selectivity towards molecular targets for specific pathologies and toxicity. Continuous efforts are thus devoted to the development of paramagnetic systems as candidate contrast agents with improved efficacy and lower toxicity.

Since the theory predicts that a high relaxivity is reached at the imaging fields (0.5 to 3 T) when the paramagnetic ion is coordinated to relatively large molecules, so that the reorientation times get longer, the traditional approach relies on the design of small size gadolinium(III) complexes that can bind non-covalently to macromolecules, in order to

\* Corresponding author at: Magnetic Resonance Center (CERM) and Interuniversity Consortium for Magnetic Resonance of Metallo Proteins (CIRMMMP), Via L. Sacconi 6, 50019 Sesto Fiorentino, Italy.

E-mail address: [luchinat@cerm.unifi.it](mailto:luchinat@cerm.unifi.it) (C. Luchinat).

<https://doi.org/10.1016/j.jmro.2020.100003>

Received 20 May 2020; Received in revised form 17 July 2020; Accepted 17 July 2020

2666-4410/© 2020 The Author(s). Published by Elsevier Inc. This is an open access article under the CC BY-NC-ND license.

(<http://creativecommons.org/licenses/by-nc-nd/4.0/>)

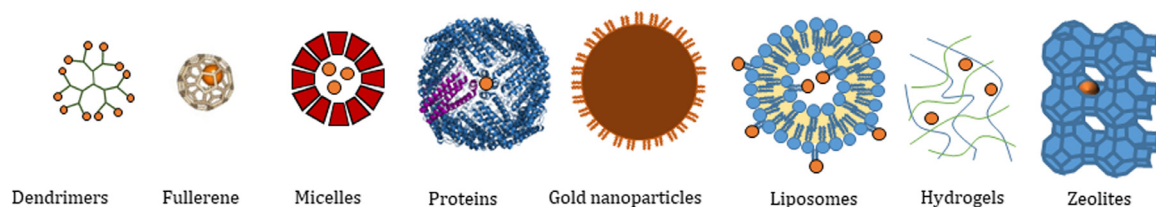


Fig. 1. Nanocarriers proposed for delivery of MRI contrast agents.

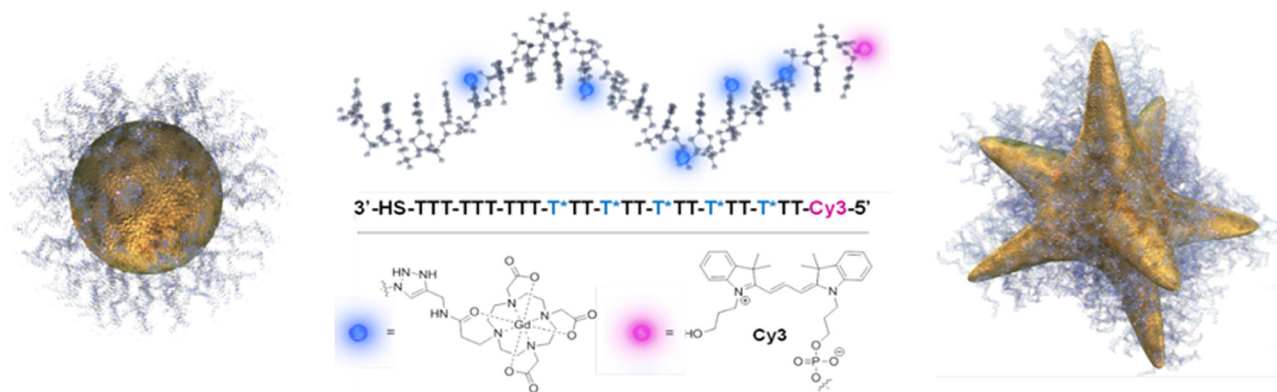


Fig. 2. Spherical and star-shaped gold nanoparticles functionalized with poly deoxy-thymine nucleotides containing conjugation sites for covalent attaching of GdDO3A complexes. Adapted from reference [19].

selectively increase their reorientation time, and thus the relaxation enhancement in the presence of the selected biological target.

One strategy of choice for the development of contrast agents with both a higher efficacy and a lower toxicity presently consists in the encapsulation of the paramagnetic complexes into biocompatible carriers able to protect their cargo [5,11,12]. High-capacity carriers that can be loaded with a huge number of paramagnetic metal ions can in fact both increase the sensitivity of MRI and monitor specific cellular targets, if functionalized to deliver the paramagnetic ions to these desired targets. Furthermore, nanoparticles that allow for a limited mobility of the paramagnetic moieties also experience relatively long reorientation time, thus appearing as ideal candidates, as long as they are small enough to pass through the vascular system and, possibly, through the breaches in the vascular endothelia that are found in some pathological conditions. Suitable nanoparticles and nanocarriers able to deliver hundreds, thousands, or even more paramagnetic ions to selected targets can be self-aggregates, nanogels, dendrimers, micelles, liposomes, proteins, viral capsids, etc. (Fig. 1) [13–17]. Since they have different properties than small molecules in biodistribution, confinement effects, surface accessible area, etc., we may expect that the development of these systems can unveil unexpected effects, some of which are already emerging.

Gold nanoparticles covered with peptides functionalized with gadolinium complexes represent a promising approach to improve relaxivity (Fig. 2) [18]. The relaxivity of a paramagnetic complex is defined as the paramagnetic enhancement of the water proton relaxation rate in the presence of 1 mM concentration of the paramagnetic ion, and it is the parameter conveniently used to describe the efficacy of a paramagnetic complex as a contrast agent. Whereas for such gold spherical nanoparticles the increase in relaxivity is in line with the expectations, when the nanoparticles are star-shaped it becomes exceptionally high (Fig. 3), much higher than what can be expected for a single water molecule regularly coordinated to the gadolinium ion [19]. The origin of this unexpected large relaxivity was proposed to be related to surface-mediated elongation of second-sphere water residence lifetimes, and thus to the reduced diffusional time of water molecules around the particle surface. The star-shape and the extended hydrophilic surface caused by the nucleotides covering the nanoparticles would thus form

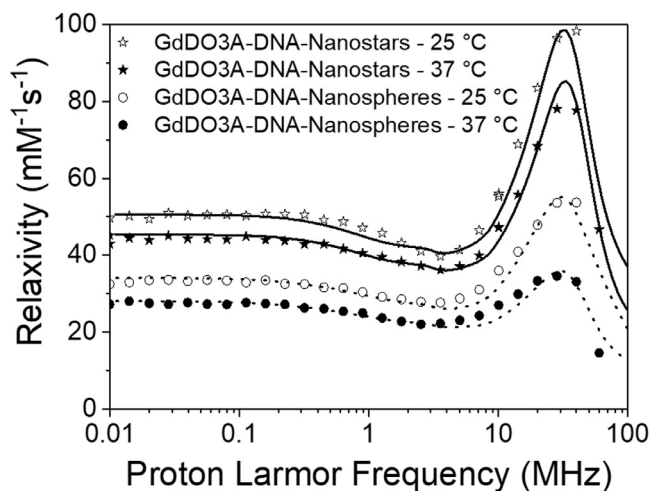


Fig. 3.  $^1\text{H}$  NMRD profiles for spherical- and star-shape Gd-based gold nanoparticles. The efficacy of the contrast agent increases with its relaxivity at the MRI magnetic field.

a sterically crowded, hydrogen-bonding-rich environment where an extended network of second-sphere water molecules can reside adjacent to the gadolinium(III) ion. However, a detailed model to describe this effect is still lacking, and a fully understanding of this process may help in the design of systems of further improved efficacy.

Along the same line, also nanodiamonds with Gd-complexes covalently coupled by amide bonds to their surface exhibit a very large relaxivity [20], which largely exceeds the value theoretically ascribable to the presence of two fast exchanging water molecules coordinated to the Gd ion, present in the synthesized compound. Again, a plausible explanation may be related to the hydrophilic, amidated carbon-based nanoparticles being able to form robust and continuous hydration layers near the nanodiamond surface.

Furthermore, first reports on contrast agents confined in nanogels also indicate extraordinarily large relaxivity enhancements [21]. Nanogels are aqueous dispersions of hydrogel particles formed by physically or chemically cross-linked nanosized polymer networks [22,23]. They are highly biocompatible, can load a high number of guest molecules, and can be functionalized to deliver their cargo at the target site, while protecting it from degradation during delivery. Also in this case the observed surprisingly large relaxivity may be linked to a highly hydrophilic environment that can drastically modify water dynamics, similarly to what happens when molecular motions are restricted in confined regions.

Since it is well known that gadolinium is toxic if freely released in the human body (a link has been recently established between Gd-containing contrast agents and nephrogenic systemic fibrosis [24,25]), many studies are now focusing to the development of manganese complexes as valid alternatives to gadolinium agents, because also manganese(II) can induce large paramagnetic relaxation rates, due to its large electron relaxation times and spin quantum number. The possibility of confinement of manganese ions inside nanocarriers, and their release in selected biological targets, may thus suggest that manganese nanostructures can be preferable to gadolinium-based systems. The relaxation enhancement presently achieved with manganese oxide nanoparticles is however smaller than that obtained with gadolinium nanoparticles [26]. Strategies to increase the amount of manganese ions at the surface of the nanoparticles and of the water molecules coordinated (or slowly diffusing) around the nanoparticles thus need to be developed. A possible approach is coating the particles with silica or other materials easily allowing access of water molecules to the manganese ions [27]. The porous coating, which enables water exchange across the shell, combined with a large surface area-to-volume ratio, is expected to increase water accessibility to the manganese core and consequently to provide enhanced relaxivity.

In summary, although the mechanisms responsible for the increase in relaxivity are well understood in homogeneous solutions, accurate models for the relaxation increase in paramagnetic nanoparticles and how their chemical structure affects the relaxivity of these systems are in large part missing yet, so that further surprises may be expected.

### 3. Hyperpolarization: from passive to active contrast, biomedical and materials applications

Another strategy that has recently revolutionized the area of molecular imaging is dissolution DNP (dDNP) [28]. In this case, the contrast agent is a specific metabolite, which is isotopically enriched in a particular position (e.g.: [ $^{13}\text{C}$ ]-pyruvate) and that is hyperpolarized prior to injection in the patient. The molecule is selected so that its metabolism is specific for a physiological or pathological tissue [29,30]. This approach has been demonstrated to yield superior resolution in determining the boundaries of the different compartments, up to the point that it has been uptaken in clinical practice [31]. In dDNP the hyperpolarization usually takes place at liquid helium temperature on 200–800  $\mu\text{l}$  samples, which are subsequent dissolved by pressurized hot water and collected for injection [28]. Working at liquid helium temperature ensures high polarization levels but, at the same time, pushes the longitudinal relaxation time of the target nuclei to impractical values (in the hours range for  $^{13}\text{C}$ ). Furthermore, most biologically-relevant liquids will undergo phase segregation during freezing (*vide infra*). Therefore, dDNP research has been oriented towards the development of new formulations, to increase the overall polarization, including: development of glassing matrices and radicals, removal of the radical after dissolution and inclusion of dopants that increase the efficiency of DNP. The latter point has recently raised a considerable interest: in 2012 the Kovacs group has demonstrated that the addition of gadolinium(III)-DOTA ions yields a 3-fold increase in the polarization in trityl-based DNP, whereas the increase is modest in the case of TEMPO-based DNP [32]. This was originally attributed to an increase of the solid-effect (SE) mechanism,

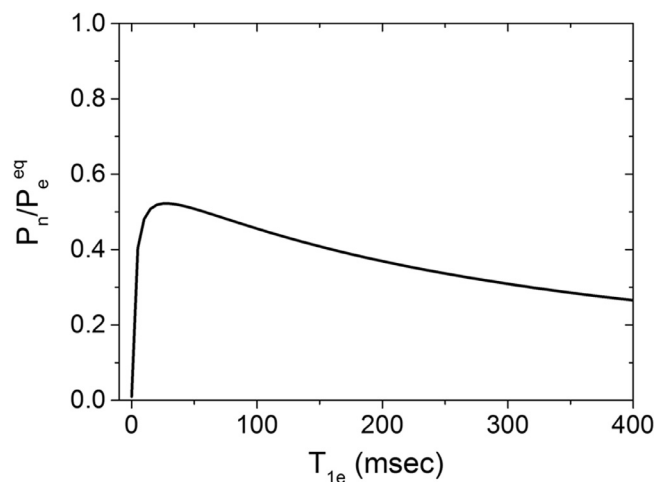


Fig. 4. The average bulk nuclear polarization normalized to the thermal equilibrium electron polarization,  $P_n/P_e^{\text{eq}}$ , as a function of  $T_{1e}$  for a total of 960  $^{13}\text{C}$  nuclei placed on a 2D grid, 6 Å apart in each direction. For the parameters of the simulation see Ref. [33]. Reproduced by permission of the PCCP owner societies.

which is expected to dominate trityl-DNP with respect to the cross-effect (CE) mechanism which is expected to dominate TEMPO-DNP. However, a detailed analysis of the DNP lineshapes based on the experimental EPR spectra of the trityl formulation with and without Gd-DOTA revealed that both mechanisms are present and that they are increased approximately by the same amount [33]. A quantum mechanical description of the ongoing processes revealed that the presence of Gd-DOTA makes electron spectral diffusion more efficient, favoring indirect CE polarization transfer: this effect arises from MW irradiation that saturate the transitions of electrons other than those at CE distance, which then indirectly depolarize the CE electron pairs (iCE-DNP) via electron spectral diffusion (eSD). At the same time, Gd-DOTA decreases electron longitudinal and transverse relaxation times by a factor 10 and 3 respectively. This impacts strongly on the saturability of the EPR line, and this explains [33] the decrease of the DNP efficiency observed in conditions other than the HYPERSENSE setup [34].

Of note, however, besides spectral diffusion, in reference [33] it is demonstrated that the presence of gadolinium(III) impacts dramatically the way spin diffusion among nuclei propagates DNP.

To demonstrate the impact of the electron relaxation time  $T_{1e}$  of a polarizing agent on the overall efficiency of the polarization transfer of its neighboring nuclei, a simple numerical model can be used: a two-dimensional grid of dipolar coupled nuclei hyperfine coupled to a single electron [35], where SE is active in a nuclear spin system with standard spin diffusion. The model simply distinguishes among (i) the nuclei that are directly polarized because of their strong hyperfine interaction, (ii) a subset of “local” nuclei that are polarized both because of direct interaction with the electron as well as because of spin diffusion from the core, and (iii) the bulk nuclei that are polarized only via spin diffusion. The core and local nuclear polarizations are generated by simulating SE, and fed into a set of coupled equations for the electron and nuclear polarizations, and the spin diffusion is introduced by introducing dipole-dipole cross relaxation rates between neighboring nuclei.

Previous work has shown that a shorter  $T_{1e}$  can be advantageous when the polarization must be transferred to many nuclei [36–40]. Following this, Fig. 4 reports the average bulk nuclear polarization normalized to the thermal equilibrium electron polarization,  $P_n/P_e^{\text{eq}}$ , as a function of  $T_{1e}$  for a total of 960  $^{13}\text{C}$  nuclei, 6 Å apart from each other, and one electron in the bottom left corner of the grid. In this simulation, the relaxation time of the core nuclei  $T_{1c}$  was taken to be 100 times longer than  $T_{1e}$  at all times, to mimic the dependence of the core nuclei

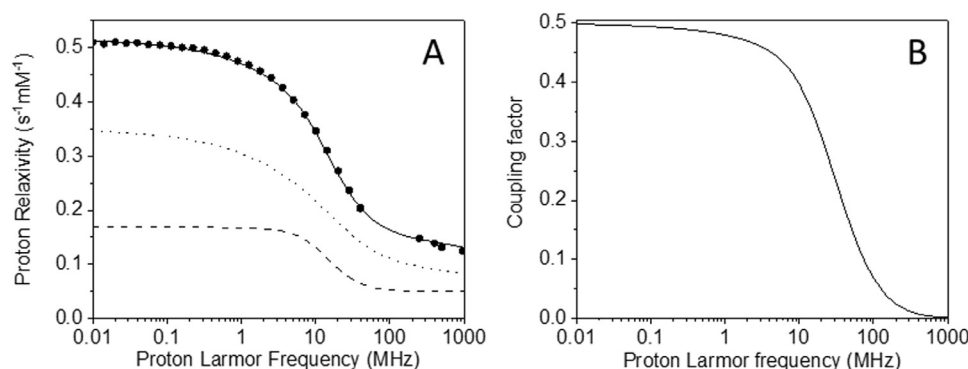


**Fig. 5.** (A) Field dependence of the water proton relaxivity for a TEMPOL solution at 298 K, analyzed using the force-free hard-sphere translational diffusion model (dotted line) and an additional contribution from rotational diffusion (dashed line), and (B) corresponding field dependence of the derived coupling factor [59].

relaxation time on the electron relaxation time. The parameters used for the simulation are given in the figure caption. This simple model cannot be used to estimate the actual experimental gain in enhancement. It however demonstrates that lowering the value of  $T_{1e}$  of the polarizing electrons results in an increase of the nuclear bulk polarization, up to a certain degree. Indeed, Fig. 4 shows that in the two dimensional spin model the decrease of  $T_{1e}$  initially increases  $P_n/P_e^{eq}$ , until a maximum is reached and then  $P_n/P_e^{eq}$  starts decreasing as  $T_{1e}$  is further decreased. This increase in polarization can be explained by the increase in the DNP turnover rate when  $T_{1e}$  is decreased, i.e. the electron must recover quickly in order to effectively transfer its polarization to many nuclei. The decrease at very short  $T_{1e}$  values is a result of the decrease in the  $T_{1c}$ , which act as a polarization “sink” for the local and bulk nuclei.

A number of computational models have recently emerged for simulating DNP in static and spinning samples [41–47] and immediately it has been recognized that the role of spin diffusion in relaying the polarization to the bulk nuclei is so important that quantitative spin-diffusion models have then been developed for a proper description of DNP, for instance including the presence of paramagnetic relaxation sinks or depolarization induced by biradicals under MAS, as well as the presence of discontinuities in the samples. The latter aspect is particularly intriguing because it allows for relating the time dependence of the buildup to the morphology and distribution of the discontinuities, also in the case where the spin diffusion is mostly occurring across surfaces [40].

In solution, the Overhauser Effect (OE) is the only active mechanism for DNP. In OE the polarization transfer from unpaired electrons to nuclei occurs through stochastic modulation of the hyperfine interaction between electron and nuclear magnetic moments [48]. Its efficacy is described by the coupling factor, corresponding to the ratio between the electron-nucleus cross relaxation rate and the nuclear longitudinal relaxation rate [49]. The sensitivity of the coupling factor to the correlation time modulating the dipole–dipole interaction has been used to obtain information on the accessibility and dynamics of the solvent molecules at the surface of macromolecules [50,51], a piece of information very important for the functional characterization of biosystems. Through the attachment of nitroxide radical spin probes to targeted sites on the biomolecule of interest (proteins, lipid vesicles, synthetic polymers, nucleic acids, etc.), the observed Overhauser DNP enhancements selectively reflect water dynamics around the spin probe, due to the distance dependence of hyperfine coupling, thus allowing for a site specific mapping of solvent mobility.

#### 4. Signal enhancements: old beliefs challenged by new experiments

The two dominating effects at low field, SE and CE, are expected to scale down with the magnetic field (even though the loss can be partly compensated with electrons whose EPR linewidths do not increase with increasing field) [52–54]. On the other hand, also OE (see above) can be very effective in insulating solids [55,56]. A very surprising, unpredicted

field dependence was observed in this respect, as the DNP enhancement was found to increase, rather than decrease, with increasing the field. A dominant contribution from Fermi-contact relaxation is expected to be responsible for the  $^1\text{H}$  DNP-MAS enhancements observed in the solid state at about 100 K and using BDPA as polarizing agent, and molecular motions occurring at DNP-relevant frequencies increase on moving to higher fields, as shown in molecular dynamics simulations, ensuring a more efficient modulation for achieving DNP [46].

The OE DNP expected for nitroxide radicals as TEMPOL or TEMPONE dissolved in water was predicted since half a century [48] to decrease with the inverse squared magnetic field when dipole-dipole relaxation is modulated by reorientational diffusion and with the inverse magnetic field to the 3/2 power when modulated by translational diffusion. Because molecular motions at room temperature occur on a timescale of tens of picoseconds, this would provide negligible enhancements at magnetic fields larger than few Tesla. Surprisingly, in the last decade it was shown that the decrease in the experimentally observed DNP enhancement at high magnetic fields is less steep than theoretically predicted [57]. It was understood that this is because the theoretical predictions assume the molecules to move rigidly during reorientational and translational diffusion, and that the unpaired electron is located at the center of a spherical molecule. These assumptions can satisfactorily model the field dependence of relaxation at low fields, but not at high fields. In fact, the presence of dynamics on a much shorter timescale plays an important role in determining the coupling factor above few Tesla, as also confirmed by molecular dynamics simulations [58]. This is because at high fields the coupling factor increases with decreasing the correlation time modulating the hyperfine interaction, i.e. in the presence of faster local mobility. Such fast dynamics is thus extremely important for an accurate estimate of the coupling factor at high fields, which is mostly sensitive to motions in the picosecond and sub-picosecond time scale, and is thus responsible for the unpredicted relatively large DNP enhancements. Furthermore, also the displacement of the unpaired electron from the center to the periphery of the molecule causes a slower decrease of the coupling factor with increasing the field, which can be modeled through the presence of shorter correlation times. Fig. 5 shows the field dependence of the coupling factor calculated for TEMPOL in water, taking into account the contributions to relaxation from translational and rotational diffusion, as detected from the field dependence of the nuclear relaxivity [59–61].

An unexpected, exceptionally large OE DNP enhancement was recently measured also for  $^{13}\text{C}$  in  $\text{CHCl}_3$  and  $\text{CCl}_4$  solutions with the radical TEMPONE as polarizing molecule, resulting in about a factor 1000 at magnetic fields of 3 Tesla and room temperature [63]. This enhancement is ascribed to Fermi-contact contributions to relaxation, resulting from unpaired electron spin density that passes from the polarizing molecule to carbon through the chlorine atoms (being present both in  $\text{CHCl}_3$  and  $\text{CCl}_4$ ). Fermi-contact relaxation may in fact increase the absolute value of the coupling factor, if the Fermi-contact relaxation rate is larger than the dipole–dipole relaxation rate, at fields  $\gamma_s/\gamma_I$  times



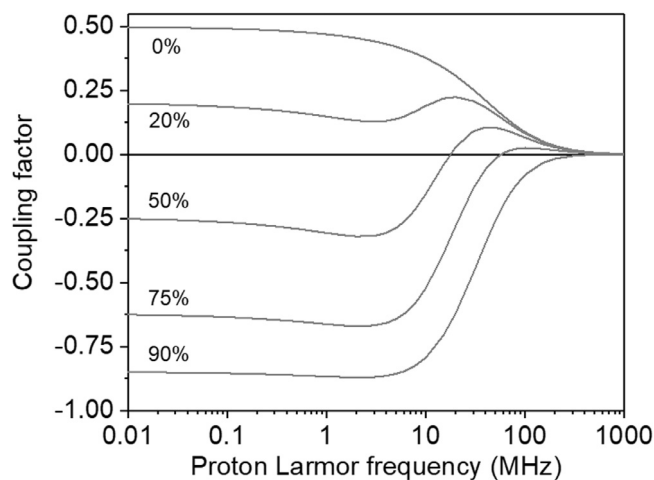


Fig. 6. Field dependence of the  $^1\text{H}$  coupling factor arising for molecules with electron-nucleus dipole-dipole interaction modulated with a translational correlation time of 30 ps and Fermi-contact interaction modulated with the same correlation time, for different amounts of the Fermi-contact relaxation with respect to the total (dipolar plus contact) paramagnetic relaxation. Adapted from [62].

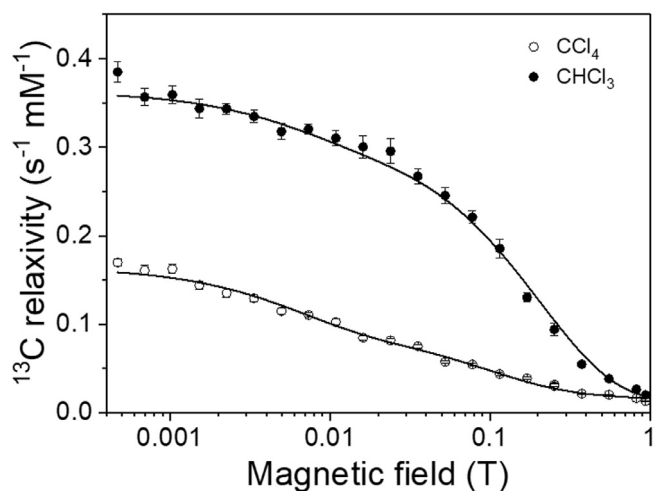


Fig. 7. The  $^{13}\text{C}$  relaxivity profiles of  $\text{CCl}_4$  and  $\text{CHCl}_3$  solutions in the presence of TEMPONE at  $25^\circ\text{C}$  [63].

smaller than the inverse of the correlation time (Fig. 6). A “pulse” model [64] was adopted to describe this effect, accounting for a Fermi-contact interaction due to random collisions occurring during molecular diffusion of the solvent molecules around the paramagnetic molecule which determine the transfer of unpaired electron spin density. This interaction is modulated with correlation times corresponding to the contact times, which in turn depend on the relative conformation of the transient complex formed by the paramagnetic molecule and the solvent molecule. The relaxation data (see Fig. 7) indicate that a distribution of contact correlation times is present, with a major fraction at about 1 ps, and minor fractions at times of tens of picoseconds or higher. Major improvements are expected in the near future by exploiting the large signal enhancements achievable both in solution and in the solid state through contact-driven relaxation mechanisms. One thousand fold enhancements of  $^{13}\text{C}$  signals at high magnetic fields open new perspectives to NMR of biomolecular systems, thanks to such impressive increase in sensitivity.

## 5. Conclusions

In conclusion, it is of capital importance in the design of the experiments to consider the nature of the system whose signal/relaxation is to be enhanced. Being able to model the diffusion properties of the system under investigation allows one to monitor specific aspects, such as the dimensions or the mobility of a particular analyte and, at the same time provides a formidable tool for improving the experimental design in a rational way.

## Declaration of Competing Interest

The authors declare that they have no known competing financial interests or personal relationships that could have appeared to influence the work reported in this paper.

## Acknowledgements

The support from Fondazione Cassa di Risparmio di Firenze, MIUR PRIN 2017A2KEPL, Ministero della Salute GR-2016-02361586, the European Commission, H2020 contract Instruct-ULTRA no. 731005, and COST EURELAX CA15209. The authors also acknowledge the support and the use of resources of Instruct-ERIC, a Landmark ESFRI project, and specifically the CERM/CIRMMF Italy Centre.

## References

- [1] Y. Shrot, L. Frydman, The effects of molecular diffusion in ultrafast two-dimensional nuclear magnetic resonance, *J. Chem. Phys.* 128 (2008) 164513 <https://doi.org/10.1063/1.2890969>.
- [2] K. Nicolay, K.P.J. Braun, R.A. de Graaf, R.M. Dijkhuizen, M.J. Kruiskamp, Diffusion NMR spectroscopy, *NMR Biomed.* 14 (2001) 94–111 <https://doi.org/10.1002/nbm.686>.
- [3] G.A. Morris, Diffusion-ordered spectroscopy, *EMagRes*, American Cancer Society, 2009 <https://doi.org/10.1002/9780470034590.emrstm0119.pub2>.
- [4] S. Caldarelli, NMR Chromatographic, a tool for the analysis of mixtures of small molecules, *Magn. Reson. Chem.* 45 (2007) S48–S55 <https://doi.org/10.1002/mrc.2143>.
- [5] J. Wahsner, E.M. Gale, A. Rodríguez-Rodríguez, P. Caravan, Chemistry of MRI contrast agents: current challenges and new frontiers, *Chem. Rev.* 119 (2019) 957–1057 <https://doi.org/10.1021/acs.chemrev.8b00363>.
- [6] V. Ntziachristos, M.A. Pleitez, S. Aime, K.M. Brindle, Emerging technologies to image tissue metabolism, *Cell Metab.* 29 (2019) 518–538 <https://doi.org/10.1016/j.cmet.2018.09.004>.
- [7] T. Lammers, S. Aime, W.E. Hennink, G. Storm, F. Kiessling, Theranostic nanomedicine, *Acc. Chem. Res.* 44 (2011) 1029–1038 <https://doi.org/10.1021/ar200019c>.
- [8] S. Aime, M. Botta, M. Fasano, E. Terreno, Lanthanide(II) chelates for NMR biomedical applications, *Chem. Soc. Rev.* 27 (1998) 19–29.
- [9] P. Caravan, Strategies for increasing the sensitivity of gadolinium based MRI contrast agents, *Chem. Soc. Rev.* 35 (2006) 512 <https://doi.org/10.1039/b510982p>.
- [10] P. Caravan, J.J. Ellison, T.J. McMurtry, R.B. Lauffer, Gadolinium(III) chelates as MRI contrast agents: structure, dynamics, and applications, *Chem. Rev.* 99 (1999) 2293–2351.
- [11] S. Aime, D.D. Castelli, S.G. Crich, E. Gianolio, E. Terreno, Pushing the sensitivity envelope of lanthanide-based Magnetic Resonance Imaging (MRI) contrast agents for molecular imaging applications, *Acc. Chem. Res.* 42 (2009) 822–831 <https://doi.org/10.1021/ar800192p>.
- [12] I. Bertini, C. Luchinat, G. Parigi, E. Ravera, NMR of paramagnetic molecules: applications to metalloproteins and models, 2017.
- [13] S. Aime, L. Frullano, S. Geninatti Crich, Compartmentalization of a gadolinium complex in the apoferritin cavity: a route to obtain high relaxivity contrast agents for magnetic resonance imaging, *Angew. Chem. Int. Ed.* 41 (2002) 1017–1019 [https://doi.org/10.1002/1521-3773\(20020315\)41:6<1017::AID-ANIE1017>3.0.CO;2-P](https://doi.org/10.1002/1521-3773(20020315)41:6<1017::AID-ANIE1017>3.0.CO;2-P).
- [14] É. Tóth, R.D. Bolskar, A. Borel, G. González, L. Helm, A.E. Merbach, B. Sitharaman, L.J. Wilson, Water-soluble gadofullerenes: toward high-relaxivity, pH-responsive MRI contrast agents, *J. Am. Chem. Soc.* 127 (2005) 799–805 <https://doi.org/10.1021/ja044688h>.
- [15] C. Platas-Iglesias, L. Vander Elst, W. Zhou, R.N. Muller, C.F.G.C. Geraldes, T. Maschmeyer, J.A. Peters, Zeolite GdNaY nanoparticles with very high relaxivity for application as contrast agents in magnetic resonance imaging, *Chem. – Eur. J.* 8 (2002) 5121–5131 [https://doi.org/10.1002/1521-3765\(20021115\)8:22<5121::AID-CHEM5121>3.0.CO;2-W](https://doi.org/10.1002/1521-3765(20021115)8:22<5121::AID-CHEM5121>3.0.CO;2-W).
- [16] F. Carniato, L. Tei, M. Cossi, L. Marchese, M. Botta, A chemical strategy for the relaxivity enhancement of Gd(III) chelates anchored on mesoporous silica nanoparticles, *Chem. – Eur. J.* 16 (2010) 10727–10734 <https://doi.org/10.1002/chem.201000499>.

- [17] F. Carniato, L. Tei, A. Arrais, L. Marchese, M. Botta, Selective anchoring of Gd<sup>III</sup> chelates on the external surface of organo-modified mesoporous silica nanoparticles: a new chemical strategy to enhance relaxivity, *Chem. – Eur. J.* 19 (2013) 1421–1428 <https://doi.org/10.1002/chem.201202670>.
- [18] M.F. Ferreira, B. Mousavi, P.M. Ferreira, C.I.O. Martins, L. Helm, J.A. Martins, C.F.G.C. Geraldes, Gold nanoparticles functionalised with stable, fast water exchanging Gd<sup>3+</sup> chelates as high relaxivity contrast agents for MRI, *Dalton Trans.* 41 (2012) 5472 <https://doi.org/10.1039/c2dt30388d>.
- [19] M.W. Rotz, K.S.B. Culver, G. Parigi, K.W. MacRenaris, C. Luchinat, T.W. Odom, T.J. Meade, High relaxivity Gd(III)–DNA gold nanostars: investigation of shape effects on proton relaxation, *ACS Nano* 9 (2015) 3385–3396 <https://doi.org/10.1021/nn5070953>.
- [20] N. Rammohan, K.W. MacRenaris, L.K. Moore, G. Parigi, D.J. Mastarone, L.M. Manus, L.M. Lilley, A.T. Preslar, E.A. Waters, A. Filicko, C. Luchinat, D. Ho, T.J. Meade, Nanodiamond–Gadolinium(III) aggregates for tracking cancer growth in vivo at high field, *Nano Lett.* 16 (2016) 7551–7564 <https://doi.org/10.1021/acs.nanolett.6b03378>.
- [21] T. Courant, V.G. Roullin, C. Cadiou, M. Callewaert, M.C. Andry, C. Portefaix, C. Hoefel, M.C. de Goltstein, M. Port, S. Laurent, L.V. Elst, R. Muller, M. Molinari, F. Chuburu, Hydrogels incorporating GdDOTA: towards highly efficient dual T1/T2 MRI contrast agents, *Angew. Chem. Int. Ed.* 51 (2012) 9119–9122 <https://doi.org/10.1002/anie.201203190>.
- [22] I. Neamt, A.G. Rusu, A. Diaconu, L.E. Nita, A.P. Chiriac, Basic concepts and recent advances in nanogels as carriers for medical applications, *Drug Deliv.* 24 (2017) 539–557 <https://doi.org/10.1080/10717544.2016.1276232>.
- [23] H. Wang, J. Qian, F. Ding, Recent advances in engineered chitosan-based nanogels for biomedical applications, *J. Mater. Chem. B* 5 (2017) 6986–7007 <https://doi.org/10.1039/C7TB01624G>.
- [24] P. Marckmann, L. Skov, K. Rossen, A. Dupont, M.B. Damholt, J.G. Heaf, H.S. Thomsen, Nephrogenic systemic fibrosis: suspected causative role of gadodiamide used for contrast-enhanced magnetic resonance imaging, *J. Am. Soc. Nephrol.* 17 (2006) 2359–2362 <https://doi.org/10.1681/ASN.2006060601>.
- [25] N. Jalandhara, R. Arora, V. Batuman, Nephrogenic systemic fibrosis and gadolinium-containing radiological contrast agents: an update, *Clin. Pharmacol. Therap.* 89 (2011) 920–923 <https://doi.org/10.1038/clpt.2010.346>.
- [26] H.B. Na, J.H. Lee, K. An, Y.I. Park, M. Park, I.S. Lee, D.-H. Nam, S.T. Kim, S.-H. Kim, S.-W. Kim, K.-H. Lim, K.-S. Kim, S.-O. Kim, T. Hyeon, Development of aT1 contrast agent for magnetic resonance imaging using MnO nanoparticles, *Angew. Chem.* 119 (2007) 5493–5497 <https://doi.org/10.1002/ange.200604775>.
- [27] T. Kim, E. Momin, J. Choi, K. Yuan, H. Zaidi, J. Kim, M. Park, N. Lee, M.T. McMahon, A. Quinones-Hinojosa, J.W.M. Bulte, T. Hyeon, A.A. Gilad, Mesoporous silica-coated hollow manganese oxide nanoparticles as positive T<sub>1</sub> contrast agents for labeling and MRI tracking of adipose-derived mesenchymal stem cells, *J. Am. Chem. Soc.* 133 (2011) 2955–2961 <https://doi.org/10.1021/ja1084095>.
- [28] J.H. Ardenkjaer-Larsen, B. Fridlund, A. Gram, G. Hansson, L. Hansson, M.H. Lerche, R. Servin, M. Thanning, K. Golman, Increase in signal-to-noise ratio of >10,000 times in liquid-state NMR, *PNAS* 100 (2003) 10158–10163 <https://doi.org/10.1073/pnas.173385100>.
- [29] S.E. Day, M.I. Kettunen, F.A. Gallagher, D.-E. Hu, M. Lerche, J. Wolber, K. Golman, J.H. Ardenkjaer-Larsen, K.M. Brindle, Detecting tumor response to treatment using hyperpolarized 13C magnetic resonance imaging and spectroscopy, *Nat. Med.* 13 (2007) 1382–1387 <https://doi.org/10.1038/nm1650>.
- [30] T. Harris, G. Eliyahu, L. Frydman, H. Degani, Kinetics of hyperpolarized 13C1-pyruvate transport and metabolism in living human breast cancer cells, *Proc. Natl. Acad. Sci. USA* 106 (2009) 18131–18136 <https://doi.org/10.1073/pnas.0909049106>.
- [31] S.J. Nelson, J. Kurhanewicz, D.B. Vigneron, P.E.Z. Larson, A.L. Harzstark, M. Ferrone, M. van Crielinge, J.W. Chang, R. Bok, I. Park, G. Reed, L. Carvajal, E.J. Small, P. Munster, V.K. Weinberg, J.H. Ardenkjaer-Larsen, A.P. Chen, R.E. Hurd, L.-I. Odegaardstuen, F.J. Robb, J. Tropp, J.A. Murray, Metabolic imaging of patients with prostate cancer using hyperpolarized [1-13C]Pyruvate, *Sci. Transl. Med.* 5 (2013) 198ra108 <https://doi.org/10.1126/scitranslmed.3006070>.
- [32] L. Lumata, M.E. Merritt, C.R. Malloy, A.D. Sherry, Z. Kovacs, Impact of Gd<sup>3+</sup> on DNP of [1-13C]pyruvate doped with trityl OX063, BDPA, or 4-oxo-TEMPO, *J. Phys. Chem. A* 116 (2012) 5129–5138 <https://doi.org/10.1021/jp302399f>.
- [33] E. Ravera, D. Shimon, A. Feintuch, D. Goldfarb, S. Vega, A. Flori, C. Luchinat, L. Menichetti, G. Parigi, The effect of Gd on trityl-based dynamic nuclear polarisation in solids, *Phys. Chem. Chem. Phys.* 17 (2015) 26969–26978 <https://doi.org/10.1039/C5CP04138D>.
- [34] S.A. Walker, D.T. Edwards, T.A. Siaw, B.D. Armstrong, S. Han, Temperature dependence of high field 13C dynamic nuclear polarization processes with trityl radicals below 35 Kelvin, *Phys. Chem. Chem. Phys.* 15 (2013) 15106 <https://doi.org/10.1039/c3cp51628h>.
- [35] D. Shimon, A. Feintuch, D. Goldfarb, S. Vega, Static <sup>1</sup>H dynamic nuclear polarization with the biradical TOTAPOL: a transition between the solid effect and the cross effect, *Phys. Chem. Chem. Phys.* 16 (2014) 6687–6699 <https://doi.org/10.1039/C3CP55504F>.
- [36] P.C.A. van der Wel, K.-N. Hu, J. Lewandowski, R.G. Griffin, Dynamic nuclear polarization of amyloidogenic peptide nanocrystals: GNNQNY, a core segment of the yeast prion protein Sup35p, *J. Am. Chem. Soc.* 128 (2006) 10840–10846 <https://doi.org/10.1021/ja0626685>.
- [37] K.-N. Hu, Polarizing agents and mechanisms for high-field dynamic nuclear polarization of frozen dielectric solids, *Solid State Nucl. Magn. Reson.* 40 (2011) 31–41 <https://doi.org/10.1016/j.snmr.2011.08.001>.
- [38] A.J. Rossini, A. Zagdoun, F. Hegner, M. Schwarzwälder, D. Gajan, C. Copéret, A. Lesage, L. Emsley, Dynamic nuclear polarization NMR spectroscopy of microcrystalline solids, *J. Am. Chem. Soc.* 134 (2012) 16899–16908 <https://doi.org/10.1021/ja308135r>.
- [39] V.K. Michaelis, A.A. Smith, B. Corzilius, O. Haze, T.M. Swager, R.G. Griffin, High-field 13C DNP with a radical mixture, *J. Am. Chem. Soc.* 135 (2013) 2935–2938 <https://doi.org/10.1021/ja312265x>.
- [40] A.C. Pinon, J. Schlagnitweit, P. Berruyer, A.J. Rossini, M. Lelli, E. Socie, M. Tang, T. Pham, A. Lesage, S. Schantz, L. Emsley, Measuring nano- to microstructures from relayed dynamic nuclear polarization NMR, *J. Phys. Chem. C* 121 (2017) 15993–16005 <https://doi.org/10.1021/acs.jpcc.7b04438>.
- [41] Y. Hovav, A. Feintuch, S. Vega, Theoretical aspects of dynamic nuclear polarization in the solid state – the solid effect, *J. Magn. Reson.* 207 (2010) 176–189.
- [42] Y. Hovav, A. Feintuch, S. Vega, Theoretical aspects of dynamic nuclear polarization in the solid state – The cross effect, *Journal of Magnetic Resonance* 214 (2012) 29–41.
- [43] Y. Hovav, A. Feintuch, S. Vega, Theoretical aspects of dynamic nuclear polarization in the solid state – the solid effect, *J. Magn. Reson.* 207 (2010) 176–189.
- [44] K.R. Thurber, R. Tycko, On mechanisms of dynamic nuclear polarization in solids, *Israel J. Chem.* 54 (2014) 39–46 <https://doi.org/10.1002/ijch.201300116>.
- [45] K.R. Thurber, R. Tycko, Theory for cross effect dynamic nuclear polarization under magic-angle spinning in solid state nuclear magnetic resonance: the importance of level crossings, *J. Chem. Phys.* 137 (2012) 084508 <https://doi.org/10.1063/1.4747449>.
- [46] S. Pylaeva, K.L. Ivanov, M. Baldus, D. Sebastiani, H. Elgabarty, Molecular mechanism of overhauser dynamic nuclear polarization in insulating solids, *J. Phys. Chem. Lett.* (2017) 2137–2142 <https://doi.org/10.1021/acs.jpclett.7b00561>.
- [47] A. Eubal, A. Leavesley, S.K. Jain, S. Han, Cross-effect dynamic nuclear polarization explained: polarization, depolarization, and oversaturation, *J. Phys. Chem. Lett.* 10 (2019) 548–558 <https://doi.org/10.1021/acs.jpclett.8b02834>.
- [48] K.H. Hauser, D. Stehlik, Dynamic nuclear polarization in liquids, *Adv. Magn. Reson.* 3 (1968) 79–139.
- [49] E. Ravera, C. Luchinat, G. Parigi, Basic facts and perspectives of Overhauser DNP NMR, *J. Magn. Reson.* 264 (2016) 78–87.
- [50] J.M. Franck, Y. Ding, K. Stone, P.Z. Qin, S. Han, Anomalous rapid hydration water diffusion dynamics near DNA surfaces, *J. Am. Chem. Soc.* 137 (2015) 12013–12023 <https://doi.org/10.1021/jacs.5b05813>.
- [51] J.M. Franck, A. Pavlova, J.A. Scott, S. Han, Quantitative cw Overhauser effect dynamic nuclear polarization for the analysis of local water dynamics, *Prog. Nucl. Magn. Reson. Spectrosc.* 74 (2013) 33–56 <https://doi.org/10.1016/j.pnmr.2013.06.001>.
- [52] B. Corzilius, A.A. Smith, A.B. Barnes, C. Luchinat, I. Bertini, R.G. Griffin, High-field dynamic nuclear polarization with high spin transition metal ions, *J. Am. Chem. Soc.* 133 (2011) 5648–5651.
- [53] B. Corzilius, V.K. Michaelis, S.A. Penzel, E. Ravera, A.A. Smith, C. Luchinat, R.G. Griffin, Dynamic nuclear polarization of 1H, 13C, and 59Co in a Tris(ethylenediamine)cobalt(III) crystalline lattice doped with Cr(III), *J. Am. Chem. Soc.* 136 (2014) 11716–11727 <https://doi.org/10.1021/ja5044374>.
- [54] A.S. Lilly Thankamony, J.J. Wittmann, M. Kaushik, B. Corzilius, Dynamic nuclear polarization for sensitivity enhancement in modern solid-state NMR, *Prog. Nucl. Magn. Reson. Spectrosc.* 102–103 (2017) 120–195 <https://doi.org/10.1016/j.pnmr.2017.06.002>.
- [55] T.V. Can, M.A. Caporini, F. Mentink-Vigier, B. Corzilius, J.J. Walish, M. Rosay, W.E. Maas, M. Baldus, S. Vega, T.M. Swager, R.G. Griffin, Overhauser effects in insulating solids, *J. Chem. Phys.* 141 (2014) 064202 <https://doi.org/10.1063/1.4891866>.
- [56] T.V. Can, Q.Z. Ni, R.G. Griffin, Mechanisms of dynamic nuclear polarization in insulating solids, *J. Magn. Reson.* 253 (2015) 23–35 <https://doi.org/10.1016/j.jmr.2015.02.005>.
- [57] J.-H. Ardenkjaer-Larsen, G.S. Boebinger, A. Comment, S. Duckett, A.S. Edison, F. Engelke, C. Griesinger, R.G. Griffin, C. Hilty, H. Maeda, G. Parigi, T. Prisner, E. Ravera, J. van Bentum, S. Vega, A. Webb, C. Luchinat, H. Schwalbe, L. Frydman, Facing and Overcoming sensitivity challenges in biomolecular NMR spectroscopy, *Angew. Chem. Int. Ed.* 54 (2015) 9162–9185 <https://doi.org/10.1002/anie.201410653>.
- [58] D. Sezer, M.J. Prandolini, T.F. Prisner, Dynamic nuclear polarization coupling factors calculated from molecular dynamics simulations of a nitroxide radical in water, *Phys. Chem. Chem. Phys.* 11 (2009) 6626–6637 <https://doi.org/10.1039/b905709a>.
- [59] P. Neugebauer, J.G. Krümmenacker, V.P. Denysenkov, G. Parigi, C. Luchinat, T.F. Prisner, Liquid state DNP of water at 9.2 T: an experimental access to saturation, *Phys. Chem. Chem. Phys.* 15 (2013) 6049 <https://doi.org/10.1039/c3cp44461a>.
- [60] P. Neugebauer, J.G. Krümmenacker, V.P. Denysenkov, C. Helmig, C. Luchinat, G. Parigi, T.F. Prisner, High-field liquid state NMR hyperpolarization: a combined DNP/NMRD approach, *Phys. Chem. Chem. Phys.* 16 (2014) 18781 <https://doi.org/10.1039/C4CP02451F>.
- [61] M. Bennati, C. Luchinat, G. Parigi, M.-T. Türke, Water proton relaxation dispersion analysis on a nitroxide radical provides information on the maximal signal enhancement in overhauser dynamic nuclear polarization experiments, *PhysChemChemPhys* 12 (2010) 5902–5910.
- [62] G. Parigi, E. Ravera, M. Bennati, C. Luchinat, Understanding Overhauser dynamic nuclear polarisation through NMR relaxometry, *Mol. Phys.* 117 (2019) 888–897 <https://doi.org/10.1080/00268976.2018.1527409>.
- [63] G. Liu, M. Levien, N. Karschin, G. Parigi, C. Luchinat, M. Bennati, One-thousand-fold enhancement of high field liquid nuclear magnetic resonance signals at room temperature, *Nat. Chem.* 9 (2017) 676–680 <https://doi.org/10.1038/nchem.2723>.
- [64] W. Müller-Warmuth, R. Vilhjalmsón, P.A.M. Gerlof, J. Smidt, J. Trommel, Intermolecular interactions of benzene and carbon tetrachloride with selected free radicals in solution as studied by <sup>13</sup>C and <sup>1</sup>H dynamic nuclear polarization, *Mol. Phys.* 31 (1976) 1055–1067 <https://doi.org/10.1080/00268977600100811>.